DE GRUYTER
OPEN

Synthesis and evaluation of radiolabeled, folic acid-PEG conjugated, amino silane coated magnetic nanoparticles in tumor bearing Balb/C mice

Javad Razjouyan,
Hamidreza Zolata,
Omid Khayat,
Fereidoun Nowshiravan,
Nami Shadanpour,
Meisam Mohammadnia

Abstract. To design a potent agent for positron emission tomography/magnetic resonance imaging (PET/MRI) imaging and targeted magnetic hyperthermia-radioisotope cancer therapy radiolabeled surface modified superparamagnetic iron oxide nanoparticles (SPIONs) were used as nanocarriers. Folic acid was conjugated for increasing selective cellular binding and internalization through receptor-mediated endocytosis. SPIONs were synthesized by the thermal decomposition of tris (acetylacetonato) iron (III) to achieve narrow and uniform nanoparticles. To increase the biocompatibility of SPIONs, they were coated with (3-aminopropyl) triethoxysilane (APTES), and then conjugated with synthesized folic acid-polyethylene glycol (FA-PEG) through amine group of (3-aminopropyl) triethoxysilane. Finally, the particles were labeled with ^{64}Cu ($t_{1/2}$ = 12.7 h) using 1,4,7,10-tetraazacyclododecane-1,4,7,10-tetraacetic acid mono (*N*-hydroxy succinimide ester) DOTA-NHS chelator. After the characterization of SPIONs, their cellular internalization was evaluated in folate receptor (FR) overexpressing KB (established from a HeLa cell contamination) and mouse fibroblast cell (MFB) lines. Eventually, active and passive targeting effects of complex were assessed in KB tumor-bearing Balb/C mice through biodistribution studies. Synthesized bare SPIONs had low toxicity effect on healthy cells, but surface modification increased their biocompatibility. Moreover, KB cells viability was reduced when using folate conjugated SPIONs due to FR-mediated endocytosis, while having little effect on healthy cells (MFB). Moreover, this radiotracer had tolerable *in vivo* characteristics and tumor uptake. In the receptor blocked case, tumor uptake was decreased, indicating FR-specific uptake in tumor tissue while enhanced permeability and retention effect was major mechanism for tumor uptake.

Key words: superparamagnetic iron oxide nanoparticles (SPIONs) • (3-aminopropyl) triethoxysilane (APTES) • poly ethylene glycol (PEG) • folic acid • KB cells • copper-64

J. Razjouyan
Department of Engineering, Garmsar Branch,
Islamic Azad University, Garmsar, Iran,
Tel.: +9891 0942 2335, Fax: 026 3446 4053,
E-mail: Razjouyan.javad@gmail.com

H. Zolata
Department of Energy Engineering and Physics,
Amirkabir University of Technology, Tehran, Iran

O. Khayat
Young Researchers and Elite Club, South Tehran Branch,
Islamic Azad University, Tehran, Iran

F. Nowshiravan
Biomedical Engineering Department,
Science and Research Branch,
Islamic Azad University, Tehran, Iran

N. Shadanpour
Nuclear Medicine Research Group,
Alborz Research Center, Karaj, Iran

M. Mohammadnia
Nuclear Engineering Department, East Tehran Branch,
Islamic Azad University, Tehran, Iran

Introduction

Nanotechnology is a new emerging science and in medicine it focuses on tumor targeting, drug delivery, controlled release, and multimodal imaging for cancer diagnosis and treatment (theranostics). There is renewed interest in using superparamagnetic iron oxide nanoparticles (SPIONs) as multifunctional platforms for *in vitro* cell purifications, cellular and molecular imaging, early tumor diagnosis and treatments [1]. Therapeutic approaches that exploit nanoparticles to deliver drugs selectively to cancer cells are currently considered one of the most promising tools in cancer therapeutics. SPIONs with appropriate surface as multifunctional carriers have been widely used for various biomedical applications owing to their biocompatibility, conjugation with targeting ligands and excellent tumor targeting. Particles with longer circulation times, and hence greater ability to target to the site of interest, should be 100 nm or less in diameter and have a hydrophilic

surface in order to reduce clearance by macrophages [2]. Nanoparticles will usually be taken up by the liver, spleen, and other parts of the reticuloendothelial system (RES) depending on their surface characteristics. Particles with more hydrophobic surfaces will preferentially be taken up by the liver, followed by the spleen and lungs. A biocompatible coating on particle surface is important for SPIONs circulation time and the stabilization of colloidal suspension. Therefore, SPIONs surface treatment with (3-aminopropyl) triethoxysilane (APTES) increases the presentation time of SPIONs in blood circulation. In addition, long-circulating nanocarriers such as polyethylene glycol (PEG) modified SPIONs can preferentially accumulate in the tumor sites through the leaky tumor vasculature by the enhanced permeability and retention (EPR) effect, known as passive targeting [3–5]. The PEG coating could enhance the compatibility between nanoparticles and aqueous medium, prevent particle surface from oxidation, reduce toxicity, and facilitate storage or transport [6]. Active targeting methods using SPIONs generally involve attaching a targeting ligand to the surface of the SPIONs' polymer coating. Folate receptors (FRs) on the cell membrane are a potential molecular target for tumor targeting because the FR is highly expressed in a number of epithelial carcinomas and the FRs provide highly selective sites that differentiate tumor cells from normal cells [7–9]. FRs are also overexpressed on activated and nonresting macrophages, although functional FRs are not expressed on resting macrophages or normal epithelial cells, which helps in targeting genetically altered cells [7]. Magnetic nanoparticles have been used extensively to investigate a wide range of biological phenomena such as tumor detection [10–16]. Copper-64 ($t_{1/2}$ = 12.7 h) is a unique isotope for radioisotope therapy which decays by β– (39%), β+/EC (61%). Well-established coordination chemistry, as well as an attractive half-life, makes this radionuclide feasible for efficient labeling with a wide variety of biomolecules such as peptides, antibodies, or nanoparticles. Copper-64 is commonly used in positron emission tomography (PET) imaging [17] because it can be produced at a high specific activity in biomedical cyclotrons [18, 19] and the chelation of ^{64}Cu to various macrocyclic chelators can provide an efficient route for radiolabeling a wide variety of macromolecules and nanoparticles [20].

Experimental

Materials

Iron(III)acetylacetonate, benzyl ether (99%), oleylamine (>70%), (3-aminopropyl) triethoxysilane (APTES), 1-ethyl-3-(-3-dimethylaminopropyl) carbodiimide hydrochloride (EDC), dimethyl sulfoxide (DMSO), *N*-hydroxy succinimide (NHS), dicyclohexyl carbodiimide (DCC), pyridine and bifunctional PEG, and other chemical reagents were purchased from Sigma-Aldrich Chemicals. 1,4,7,10-Tetraazacyclododecane-1,4,7,10-tetraacetic acid mono (*N*-hydroxy succinimide ester) (DOTA-NHS) was purchased from Macrocyclics Inc. Copper-64 was produced on AMIRS Cyclon 30, IBA cyclotron.

Synthesis and surface modification of SPIONs

SPIONs were synthesized through thermal decomposition method [21–24]. Briefly, 1.4 g of tris (acetylacetonato) iron (III) [Fe (acac)$_3$] was dissolved in a mixture of benzyl ether and oleylamine (20 ml/20 ml). The solution was dehydrated at 120°C for 1 h and quickly heated to 290°C for 2 h. After cooling, 65 mL of ethanol was added to the mixture. The precipitate was collected by centrifugation at 5000 rpm followed by washing in ethanol thrice. Final product was redispersed in hexane and stored at 4°C. Amino groups in the SPIONs were introduced by the reaction of the SPIONs with APTES via the replacement of alkoxide groups by hydroxyl groups to form reactive silanol group [7].

Synthesis of FA-PEG and FA-PEG-SPIONs

Folic acid was conjugate to PEG using DCC/NHS as activation agents. Briefly, 100 mg folic acid was activated in DMSO by 100 mg DCC and 55 mg NHS for 12 h at room temperature. Activated folic acid was coupled to amine groups of NH$_2$-PEG-COOH using pyridine at room temperature for 6 h followed by dialysis using Spectra/Por (molecular weight cut-off 1 kDa) and followed by lyophilization [7]. Synthesized FA-PEG (230 mg) was conjugated to amine-terminated of APTES-coated SPIONs (46 mg) using EDC/NHS at room temperature for 12 h followed by dialysis against water at 4°C for 48 h and lyophilization.

Radiolabeling of modified SPIONs with copper-64

DOTA-NHS-ester (3.5 mg) in 1 mL of PBS (pH 7.5, 1 mM) was reacted with 3.75 mL of FA-PEG-SPIONs (65 mg) overnight at 4°C. DOTA-SPIONs were separated from excess DOTA-NHS-ester by dialysis for 48 h at 4°C using 2 L of PBS. Synthesized DOTA-SPIONs (8 mg in 600 μl) were incubated with ^{64}CuCl$_2$ (74 MBq) in 0.1 M ammonium acetate buffer (pH 5.5) at 35°C for 90 min in a thermomixer. The solution was mixed with 10 μl of EDTA (10 mM) and was incubated for another 10 min. It was passed through PD10 columns (Amersham) to remove excess unbound ^{64}Cu. Radiolabeling yield was determined by thin layer chromatography (TLC). Briefly, small amount of ^{64}Cu labeled SPIONs was applied to an SG plate and developed using a 1:1 mixture (v/v) of 10% (w/v) ammonium acetate and methanol. The radioactivity in the TLC plate was measured using a Bioscan scanner (Bioscan Inc.). The nanoparticle solution was then diluted with PBS to obtain suitable doses for biodistribution studies. Synthesis steps are demonstrated in Fig. 1.
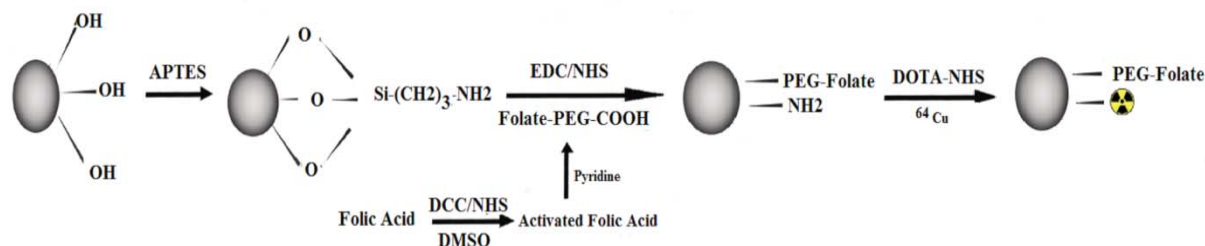
Fig. 1. Synthesis steps of ^{64}Cu-labeled, APTES-coated, PEG-FA conjugated SPIONs.

In vitro cytotoxicity studies

Mouse fibroblasts (MFCs) and folate receptor (FR) overexpressing KB cell lines were seeded in 96-well plates at 10^4 cells/well and incubated for 24 h. The cells were grown and maintained in DMEM (Dulbecco's Modified Eagle's Medium) supplemented with 10% fetal bovine serum (FBS) incubated in a humidified atmosphere (95% air and 5% CO_2) at 37°C. After a 24 h incubation period, medium containing control cells, bare SPIONs, and modified SPIONs (0.2 mM iron) was added to the wells and cells were incubated at 37°C for 1 h. The medium was then extracted, and the cells were allowed to rest. At 24 h post-treatment, the cell viability was assessed by 3-(4,5-dimethylthiazol-2-yl)-2,5-diphenyltetrazolium bromide MTT assay and using an ELISA reader (microreader, Hyperion) at 545 nm.

Biodistribution studies

In order to carry out biodistribution studies of complex, ^{64}Cu-labeled SPIONs (3.7 MBq, 0.4 mg Fe) in 100 μL of PBS were injected intravenously via the tail vein into KB tumor-bearing Balb/C mice (20–25 g, 6–8 weeks old, 0.5 cm tumor volume, $n = 5$). The mice were sacrificed at 4, 24, 48, and 72 h after injection. Animal organs were removed and weighed, and the amount of incorporated ^{64}Cu was measured by the determination of area under the curve of 511 keV peaks using a HPGe gamma detector (Canberra). FRs blockade experiments were performed at 4 and 24 h after injection, with mice injected with excess folic acid (150 μg). The activities present in the harvested organs (blood, liver, spleen, kidney, stomach, intestine, muscle, heart, lung, and tumor) were compared with the percentage of injected activity per gram of organ (% ID·g^{-1}). All animal experiments were performed in compliance with the regulations of our institution for animal experiments.

Results

Nanoparticles characterization

APTES-coated SPIONs used in this experiment were monodisperse (Fig. 2A) having an average diameter of 14 nm as determined by transmission electron microscope – TEM (Zeiss). Moreover, it was found that DOTA-SPIONs could be labeled with a yield of 96 ± 1.3%. Figure 2B shows the TLC pattern of ^{64}Cu-labeled modified SPIONs. The stability of ^{64}Cu-SPIONs was determined by incubating labeled nanoparticles in PBS and mouse serum at 4°C and 37°C, respectively, with constant shaking up to 24 h. The samples were subjected to frequent TLC analysis to measure the amount of activity dissociated from ^{64}Cu-SPIONs. *In vitro* stability of complex in PBS and serum was 93.6 ± 1.2% and 85.3 ± 2.6%, respectively. In addition, the sizes of modified SPIONs were little increased up to 4 weeks at 4°C (data not shown), confirming stable particles size and dispersion.

In vitro and *in vivo* assays

Influence of bare and APTES-treated, PEG-FA conjugated SPIONs on fibroblast cell viability at 24 h post-treatment is shown in Fig. 3. Synthesized
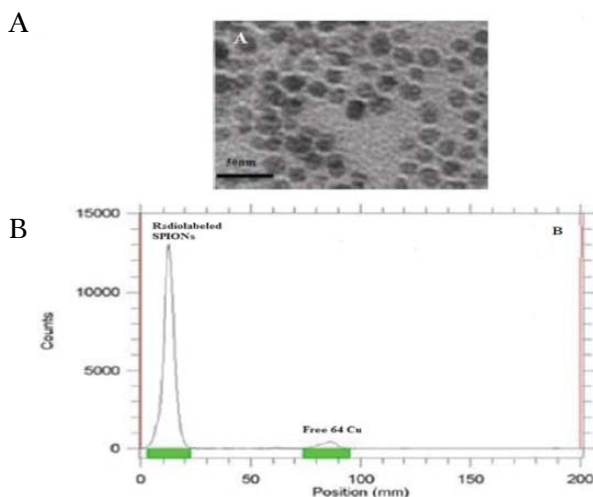

Fig. 2. (A) TEM image of SPION, (B) radiolabeling yield (96%) of ^{64}Cu-labeled modified SPIONs.
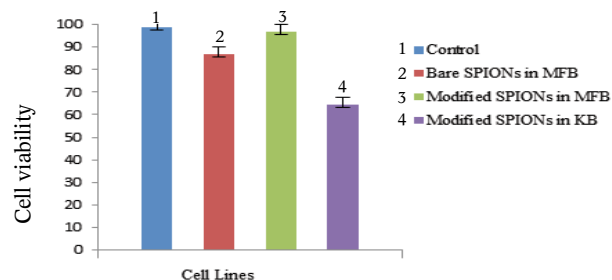

Fig. 3. Viability of MFB and KB cells determined by MTT assay after 24 h incubation with SPIONs. Each data represents the mean ± SD of three experiments.

bare SPIONs have low toxicity effects (cell viability was reduced to 86.7% in healthy cells) as shown in Fig. 3 (no. 2, red), but surface modification with appropriate coating (APTES and PEG) prevented cytotoxic effect. Modified SPIONs are more biocompatible than bare SPIONs (cell viability was reduced to 96.7% in healthy cells) as shown in Fig. 3 (no. 3, green). Moreover, KB cells viability was reduced when using folate-conjugated SPIONs due to FR-mediated endocytosis, while having little effect on healthy mouse fibroblast cell (MFB). Moreover, the biodistribution of ^{64}Cu-labeled, APTES-coated, PEG-FA conjugated SPIONs in tumor bearing Balb/C mice were studied. Radiolabeled nanoparticles were injected to tail vein and then, accumulation in major organs was investigated. The results of biodistribution and tumor/organs uptake ratios in folate targeting are given in Fig. 4 (A and B), whereas the results of blockade studies are given Fig. 4C and D.

Discussion

The FRs are emerging as a promising tumor-associated targets. The FR-specific accumulation of radiolabeled surface modified nanoparticles in normal and tumor organs was evaluated. This radiotracer allowed highly specific radiolabeling and tolerable *in vivo* characteristics with good tumor uptake. High retention of radioactivity in kidneys is a critical issue of FR targeting strategy in general. Because FRs are expressed on the luminal side of brush border membrane, they are exposed to the high folate conjugate concentration in the primary urine [25]. As a consequence, folate is significantly and specifically accumulated in the renal tissues. High binding and uptake of radioactivity into the renal tissue is a logical consequence of FR expression in proximal tubule cells, which is particularly undesirable regarding the development of therapeutic radiofolates [25].

When receptors were blocked, tumor uptake at 4 and 24 h postinjection decreased from 3.98 ± 0.24% and 5.42 ± 0.44% ID/g to 2.02 ± 0.48% and 1.86 ± 0.58% ID/g, respectively, indicating FR-specific uptake in tumor tissue. In addition, tumor/muscle ratio was reduced to half in comparison with FR targeting at 24 h postinjection. In the absence of folate targeting, EPR effect of nanoparticles is the major mechanism of uptake. Radioactivity accumulation in tumor was high at 48 and 72 h after injection (5.1 ± 0.47% and 3.1 ± 0.48% ID/g). Maximal tumor
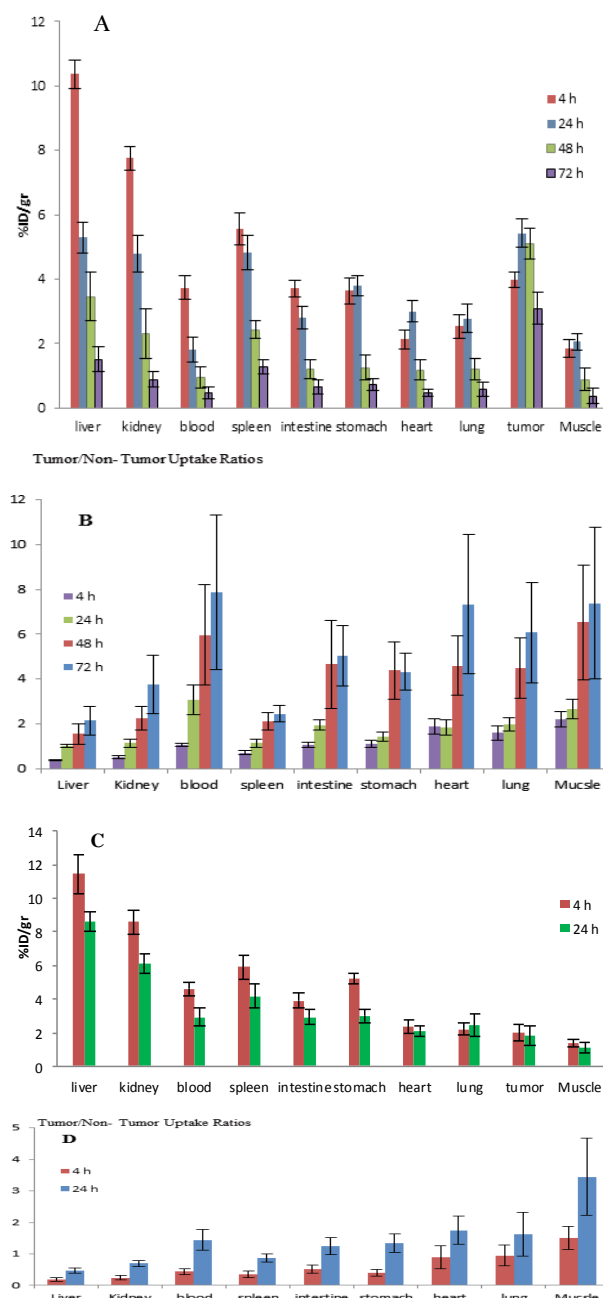
Fig. 4. (A) Biodistribution results of radiolabeled SPIONs at different times and (B) tumor/organs uptake ratios in tumor bearing Balb/C mouse. (C) Biodistribution results of radiolabeled SPIONs at different times and (D) tumor/organs ratio in (FRs blockade) tumor bearing Balb/c mouse. Data are presented as mean ± SD (*n* = 5).

Table 1. Comparison between obtained biodistribution results (1 and 2) and previous [26] biodistribution results (3 and 4)

Organ	(1) % ID/g at 4 h	(2) % ID/g at 24 h	(3) % ID/g at 4 h	(4) % ID/g at 24 h
Liver	10.36 ± 0.46	5.29 ± 0.49	33.8 ± 2.6	21.5 ± 2.9
Kidney	7.76 ± 0.36	4.796 ± 0.58	7.9 ± 0.8	8.5 ± 1.3
Blood	3.74 ± 0.38	1.82 ± 0.38	2.5 ± 0.3	2.6 ± 0.6
Spleen	5.56 ± 0.48	4.828 ± 0.53	8.8 ± 0.5	4.7 ± 1.0
Heart	2.14 ± 0.30	3.00 ± 0.32	3.7 ± 0.3	4.3 ± 0.5
Lung	2.54 ± 0.36	2.78 ± 0.43	14.4 ± 5.9	10.8 ± 1.4
Muscle	1.84 ± 0.24	5.42 ± 0.44	0.9 ± 0.2	1.0 ± 0.1
Tumor	3.98 ± 0.27	2.06 ± 0.27	5.9 ± 2.8	2.9 ± 3.1

accumulation was observed after 24 h (5.42 ± 0.44% ID/g). Clearance from the blood was fast, leading to increased tumor-to-blood ratios of radioactivity over a time (from 1.07 ± 0.06% at 4 h to 8.09 ± 2.69% at 72 h after injection). The accumulation of radioactivity in kidneys decreased to 4.8 ± 0.58 and 2.3 ± 0.78% ID/g, at 24 and 48 h after injection, respectively. Comparison between biodistribution results of our work and ^{64}Cu-labeled folate-conjugated shell cross-linked nanoparticles experiment [26] is shown in Table 1. In comparison with [19] experiment (^{64}Cu labeled magnetic nanoparticles), blood uptake increased from 1.1 ± 0.05% to 1.8% ID/g. While liver and kidney uptakes were decreased from 31.33 ± 2.33% and 6.20 ± 0.38% to 5.29 ± 0.49% ID/g and 4.8 ± 0.58% ID/g at 24 h after injection due to appropriate nanoparticles surface modifications. These modifications lead to escape of SPIONs from RES. Comparing to our previous ^{64}Cu-labeled, antibody conjugated magnetic nanoparticles experiment [27], tumor uptake and tumor/liver, tumor/kidney, tumor/blood ratios decreased from 12.5 ± 1.2%, 1.32 ± 0.10%, 1.83 ± 0.14%, 4.63 ± 0.64% to 5.29 ± 0.49%, 1.03 ± 0.08%, 1.15 ± 0.18%, 3.08 ± 0.67% at 24 h postinjection. Although tumor/organs ratios and tumor uptakes are smaller than antibody-conjugated SPIONs, folic acid-coated SPIONs are less expensive and can be prepared with relative ease.

Conclusion

Nanoparticles are well suited to design bioprobes, because of their relatively large surface area which permits high specific activity labeling and also increases payload of targeting ligands. Folic acid was conjugated on the surface of nanoparticles through PEG attachment for the effective targeting of FR-positive tumor cells. The results of MTT assay showed the influence of APTES-treated, PEG-FA-conjugated SPIONs on cancer cell death while they had small cytotoxic effect on healthy cells. The selective tumor localization of PEG-FA-treated nanoparticles should be mostly attributable to their long residence in blood circulation, leakage of blood vessels in tumors, and FR endocytosis. Therefore, our biocompatible ^{64}Cu-labeled, APTES-coated, PEG-FA-conjugated SPIONs could serve as nanoplatforms in tumor targeting.

List of abbreviations

APTES   – (3-aminopropyl) triethoxysilane,
DCC   – dicyclohexyl carbodiimide,
DMSO   – dimethyl sulfoxide,
DOTA-NHS   – 1,4,7,10-tetraazacyclododecane-1, 4,7,10-tetraacetic acid mono (*N*-hydroxy succinimide ester),
EDC   – 1-ethyl-3-(-3-dimethylaminopropyl) carbodiimide hydrochloride,
EDTA   – ethylenediaminetetraacetic acid,
EPR effect   – enhanced permeation and retention effect,
FA-PEG   – folic acid-poly ethylene glycol,
FRs   – folate receptors,
MFB   – mouse fibroblast cell,
NHS   – *N*-hydroxysuccinimide,
RES   – reticuloendothetial system,
SPIONs   – super paramagnetic iron oxide nanoparticles.

References

1. Ting-Jung, C., Tsan-Hwang, C., Chiao-Yun, C., Sodio, C., & Hsu, N. (2009). Targeted herceptin-dextran iron oxide nanoparticles for noninvasive imaging of HER2/neu receptors using MRI. *J. Biol. Inorg. Chem.*, *14*, 253–260. DOI: 10.1007/s00775-008-0445-9.

2. Brannon-Peppas, L., & Blanchette, J. O. (2012). Nanoparticle and targeted systems for cancer therapy. *J. Adv. Drug Deliv. Rev.*, *64*, 206–212. DOI: 10.1016/j.addr.2012.09.033.

3. Guo, M., Que, C., Wang, C., Liu, X., Yan, H., & Liu, K. (2011). Multifunctional superparamagnetic nanocarriers with folate-mediated and pH-responsive targeting properties for anticancer drug delivery. *Biomaterials*, *32*, 185–194. DOI: 10.1016/j.biomaterials.2010.09.077.

4. Maeda, H., & Matsumura, Y. (1989). Tumouritropic and lymphotropic principles of macromolecular drugs. *Crit. Rev. Ther. Drug Carr. System*, *6*, 193–210.

5. Ohtsuka, N., Konno, T., Miyauchi, Y., & Maeda, H. (1987). Anticancer effects of arterial administration of the anticancer agent SMANCS with lipiodol on metastatic lymph nodes. *Cancer*, *59*, 1560–1565. DOI: 10.1002/1097-0142(19870501)59:93.0.CO; 2-J.

6. Feng, B., Hong, R. Y., Wang, L. S., Guoc, L., Li, H. Z., Dingd, J., Zhenge, Y., & Wei, D. G. (2008). Synthesis of Fe3O4/APTES/PEG diacid functionalized magnetic nanoparticles for MR imaging B. *Colloid. Surf. A-Physicochem. Eng. Asp.*, *328*, 52–59. DOI: 10.1016/j.colsurfa.2008.06.024.

7. Yoo, M. K., Park, I. K., Lim, H. T., Lee, S. J., Jiang, H. L., Kim, Y. K., Choi, Y. J., Cho, M. H., & Cho, C. S. (2012). Folate-PEG-superparamagnetic iron oxide nanoparticles for lung cancer imaging. *Acta Biomater.*, *8*, 3005–3013. DOI: 10.1016/j.actbio.2012.04.029.

8. Chem, T. J., Cheng, T. W., Hung, Y. C., Lin, K. T., Liu, G. C., & Wang, Y. M. (2008) Targeted folic acid-PEG nanoparticles for noninvasive imaging of folate receptor by MRI. *J. Biomed. Mater. Res. Part A*, *87*, 165–75. DOI: 10.1002/jbm.a.31752.

9. Sun, C., Sze, R., & Zhang, M. Q. (2006). Folic acid-PEG conjugated superparamagnetic nanoparticles for targeted cellular uptake and detection by MRI. *J. Biomed. Mater. Res. Part A*, *78*(3), 550–557. DOI: 10.1002/jbm.a.30781.

10. Walczak, P., Kedziorek, D. A., Gilad, A. A., Barnett, B. P., & Bulte, J. W. (2007). Applicability and limitations of MR tracking of neural stem cells with asymmetric cell division and rapid turnover. *Magn. Reson. Med.*, *58*, 261–269. DOI: 10.1002/mrm.21412.

11. Montet, X., Montet-Abou, K., Reynolds, F., Weissleder, R., & Josephson, L. (2006). Nanoparticle imaging of integrins on tumor cells. *Neoplasia*, *8*, 214–222. DOI: 10.1593/neo.05769.

12. Lee, J. H., Huh, Y. M., Jun, Y. W., Seo, J. W., Jang, J. T., Song, H. T., Kim, S., Cho, E. J., Yoon, H. G., Suh, J. S., & Cheon, J. (2007). Artificially engineered magnetic nanoparticles for ultra-sensitive molecular imaging. *Nat. Med.*, *13*, 95–99. DOI: 10.1038/nm1467.

13. Fukukawa, K., Rossin, R., Hagooly, A., Pressly, E. D., Hunt, J. N., Messmore, B. W., Wooley, K. L., Welch, M. J., & Hawker, C. J. (2008). Synthesis and characterization of core-shell star copolymers for *in vivo* PET imaging applications. *Biomacromolecules*, *9*, 1329–1339. DOI: 10.1021/bm7014152.

14. Rossin, R., Muro, S., Welch, M. J., Muzykantov, V. R., & Schuster, D. P. (2008). *In vivo* imaging of ^{64}Cu-labeled polymer nanoparticles targeted to the lung endothelium. *J. Nucl. Med.*, *49*, 103–111. DOI: 10.2967/jnumed.107.045302.

15. Sun, G., Hagooly, A., Xu, J., Nystrom, A. M., Li, Z., Rossin, R., Moore, D. A., Wooley, K. L., & Welch, M. J. (2008). Facile, efficient approach to accomplish tunable chemistries and variable biodistributions for shell crosslinked nanoparticles. *Biomacromolecules*, *9*, 1997–2006. DOI: 10.1021/bm800246x.

16. Sun, X., Rossin, R., Turner, J. L., Becker, M. L., Joralemon, M. J., Welch, M. J., & Wooley, K. L. (2005). An assessment of the effects of shell cross-linked nanoparticle size, core composition, and surface PEGylation on *in vivo* biodistribution. *Biomacromolecules*, *6*, 2541–2554. DOI: 10.1021/bm050260e.

17. Sun, X., & Anderson, C. (2004). Production and applications of copper-64 radiopharmaceuticals. *Method. Enzymol.*, *386*, 237–261. DOI: 10.1016/S0076-6879(04)86011-7.

18. McCarthy, D., Shefer, R., Klinkowstein, R., Bass, L., Margeneau, W., Cutler, C., Anderson, C., & Welch, M. (1997). Efficient production of high specific activity ^{64}Cu using a biomedical cyclotron. *Nucl. Med. Biol.*, *24*, 35–43. DOI: 10.1016/S0969-8051(96)00157-6.

19. McCarthy, D., Bass, L., Cutler, P., Shefer, R., Klinkowstein, R., Herrero, P., Lewis, J., Cutler, C., Anderson, C., & Welch, M. (1999). High purity production and potential applications of copper-60 and copper-61. *Nucl. Med. Biol.*, *26*, 351–358. DOI: 10.1016/S0969-8051(98)00113-9.

20. Glaus, C., Rossin, R., Welch, M. J., & Gang, Bao (2010). *In vivo* evaluation of ^{64}Cu-labeled magnetic nanoparticles as a dual-modality PET/MR imaging agent. *Bioconjug. Chem.*, *21*(4), 715–722. DOI: 10.1021/bc900511j.

21. Heidari Majd, M., Asgari, D., Barara, J., Valizadeh, H., Kafil, V., Abadpour, A., Moumivand, E., Shahbazi Mojarrad, J., Rashidi, M. R., Coukos, G., & Omidi, Y. (2013). Tamoxifen loaded folic acid armed PEGylated magnetic nanoparticles for targeted imaging and therapy of cancer. *J. Colloid. Surf. B-Biointerfaces*, *106*, 117–125. DOI: 10.1016/j.colsurfb.2013.01.051.

22. Yang, X., Hong, H., Grailer, J. J., Rowland, I. J., Javadi, A., Hurley, S. A., Xiao, Y., Yang, Y., Zhang, Y., Nickles, R. J., Cai, W., Steeber, D. A., & Gonge, S. (2011). RGD-functionalized, DOX-conjugated, and ^{64}Cu-labeled superparamagnetic iron oxide nanoparticles for targeted anticancer drug delivery and SPECT/MR imaging. *J. Biomater.*, *32*(17), 4151–4160. DOI: 10.1016/j.biomaterials.2011.02.006.

23. Xu, Z., Shen, C., Hou, Y., Gao, H., & Sun, S. (2009). Oleylamine as both reducing agent and stabilizer in a facile synthesis of magnetite nanoparticles. *J. Chem. Mater.*, *21*, 1778–1780. DOI: 10.1021/cm802978z.

24. Xie, J., Xu, C., Xu, Z., Hou, Y., Young, K. L., Wang, S. X., Pourmand, N., & Sun, S. (2006). Linking hydrophilic macromolecules to monodisperse magnetite (Fe_3O_4) nanoparticles via trichloro-s-triazine. *J. Chem. Mater.*, *18*(3), 5401–5403. DOI: 10.1021/cm061793c.

25. Müller, C., Forrer, F., & Schibli, R. (2008). SPECT study of folate receptor-positive malignant and normal tissues in mice using a novel ^{99m}Tc-radiofolate. *J. Nucl. Med.*, *49*, 310–317. DOI: 10.2967/jnumed.107.045856.

26. Rossin, R., Pan, D., Qi, K., Turner, J. L., Sun, X., Wooley, K. L., & Welch, M. J. (2005). ^{64}Cu-labeled folate-conjugated shell cross-linked nanoparticles for tumor imaging and radiotherapy: synthesis, radiolabeling, and biologic evaluation *J. Nucl. Med.*, *46*, 1210–1218.

27. Zolata, H., Afarideh, H., & Abbasi-Davani, F. (2014). Radio-immunoconjugated, Dox-loaded, surface-modified superparamagnetic iron oxide nanoparticles (SPIONs) as a bioprobe for breast cancer tumor theranostics. *J. Radioanal. Nucl. Chem.*, *301*, 451–460. DOI: 10.1007/s10967-014-3101-6.